Supporting Information

Oxidant-Activated Reactions of Nucleophiles with Silicon Nanocrystals

Mita Dasog,*[1,2] Jonathan R. Thompson,[3] Nathan S. Lewis*[1,4,5]

[1]Division of Chemistry and Chemical Engineering, 210 Noyes Laboratory, California Institute of Technology, Pasadena, CA, USA

[2]Department of Chemistry, Dalhousie University, Halifax, NS, Canada

[3]Division of Engineering and Applied Sciences, California Institute of Technology, Pasadena, CA, USA

[4]Kavli Nanoscience Institute, California Institute of Technology, Pasadena, CA, USA

[5]Beckman Institute, California Institute of Technology, Pasadena, CA, USA

*Corresponding Author: nslewis@caltech.edu, mita.dasog@dal.ca

Table of Contents

Experimental details 3

Figure S1. High resolution transmission-electron micrographs of oxide-embedded Si-NCs obtained by processing $(HSiO_{1.5})_n$ polymer at (A) 1100 °C, (B) 1200 °C, and (C) 1300 °C. (Scale bar = 5 nm). 5

Figure S2. TEMs of hydrogen terminated Si-NCs liberated from composites obtained at (A) 1100°C, (B) 1200 °C, and (C) 1300 °C (Scale bar = 30 nm). Representative, (D) FT-IR and (E) high resolution XP spectra of Si 2p and O 1s regions of hydrogen terminated Si-NCs. The XP spectra are normalized for the same counts. 6

Figure S3. FT-IR spectra of 3 nm, 5 nm, and 8 nm Si-NCs after the (A) acetylferrocenium- and (B) 1,1'-diacetylferrocenium-activated methoxylation reaction. 7

Figure S4. PL spectra 3 nm (blue line), 5 nm (green line), and 8 nm (red line) of methoxylated Si-NCs with λ_{ex} = 325 nm. 8

Figure S5. FT-IR spectrum of butoxy-functionalized Si-NCs. 9

Figure S6. FT-IR spectrum of hydrogen-terminated Si-NCs reacted with butanol in the absence of ferrocenium. 10

Figure S7. FT-IR spectrum of butylamine-functionalized Si-NCs. 11

Figure S8. FT-IR spectrum of hydrogen-terminated Si-NCs reacted with butylamine in the absence of ferrocenium. 12

Figure S9. FT-IR spectrum of butanoic acid-functionalized Si-NCs. 13

Figure S10. FT-IR spectrum of hydrogen-terminated Si-NCs reacted with butanoic acid in the absence of ferrocenium. 14

Figure S11. FT-IR spectrum of butylthiol-functionalized Si-NCs..... 15

Figure S12. FT-IR spectrum of hydrogen-terminated Si-NCs reacted with dibutyl disulfide in the absence of ferrocenium. 16

Figure S13. FT-IR spectrum of diethyl phosphine-functionalized Si-NCs..... 17

Figure S14. Photographs of phosphine-stabilized Si-NCs in hexanes, before (left) and after (right) exposure to air. 18

Figure S15. FT-IR spectrum of hydrogen-terminated Si-NCs reacted with diethyl phosphine in the absence of ferrocenium. 19

Figure S16. PL spectra of hydrogen-terminated 3.1 nm (blue line), 5.2 nm (green line), and 8.0 nm (red line) Si-NCs with λ_{ex} = 325 nm. 20

Figure S17. Photographs of butylamine-stabilized Si-NCs in THF, two weeks after functionalization. The NCs on the left were functionalized in the presence of ferrocenium whereas the NC's in the photo on the right were reacted in absence of ferrocenium. 21

Figure S18. HR XP spectra of O 1s region of (A) butylthiol, (B) butylamine, and (C) diethylphosphine functionalized Si-NCs. The peaks are normalized for same counts. 22

Experimental details

Preparation of oxidants $(CpCOCH_3)CpFe^+$ or $(CpCOCH_3)_2Fe^+$

Acetylferrocenium $(CpCOCH_3)CpFe^+$, and 1,1'-diacetylferrocenium $(CpCOCH_3)_2Fe^+$, were generated in CH_3OH containing 1.0 M $LiClO_4$ (battery grade, Sigma-Aldrich) from acetylferrocene and 1,1'-diacetylferrocene, respectively, by controlled-potential electrolysis at a Pt mesh working electrode with a Pt mesh counter electrode located in a compartment separated from the working electrode by a Vycor frit. The electrolysis was performed at +0.50 V (acetylferrocene) or +0.90 V (1,1'-diacetylferrocene) vs. a Pt pseudo-reference electrode, and sufficient current was passed to generate 1.0 mM oxidant. The oxidant was used within 1 min of its generation.

Purification of Si-NCs functionalized with various nucleophiles.

Nucleophile	Solvent mixture
Butylamine	Ethanol (8.0 mL), toluene (0.5 mL), and methanol (2.5 mL)
Butanoic acid	Ethanol (10.0 mL), toluene (0.5 mL), and methanol (1.0 mL)
Butanol	Ethanol (8.0 mL), toluene (0.5 mL), and methanol (2.5 mL)
Dibutyl disulfide	Ethanol (10.0 mL), toluene (0.5 mL), and acetone (1.0 mL)

Figure S1. High resolution transmission-electron micrographs of oxide-embedded Si-NCs obtained by processing $(HSiO_{1.5})_n$ polymer at (A) 1100 °C, (B) 1200 °C, and (C) 1300 °C. (Scale bar = 5 nm).

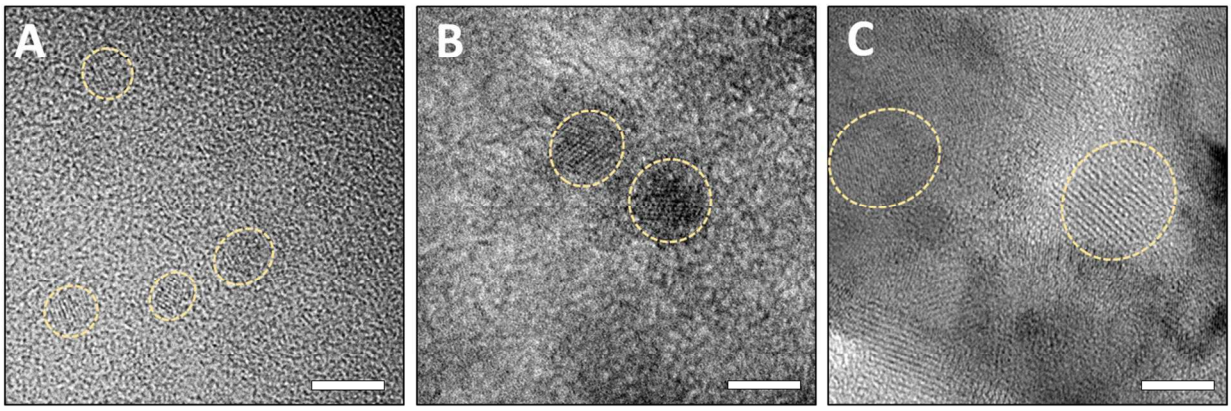

Figure S2. TEMs of hydrogen terminated Si-NCs liberated from composites obtained at (A) 1100°C, (B) 1200 °C, and (C) 1300 °C (Scale bar = 30 nm). Representative, (D) FT-IR and (E) high resolution XP spectra of Si 2p and O 1s regions of hydrogen terminated Si-NCs. The XP spectra are normalized for the same counts.

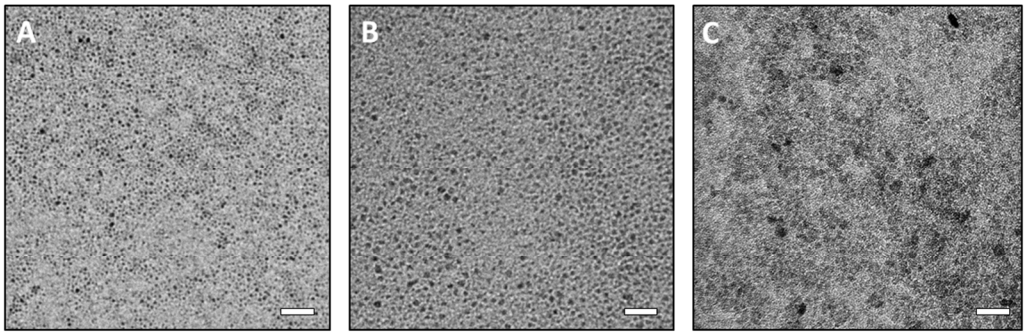

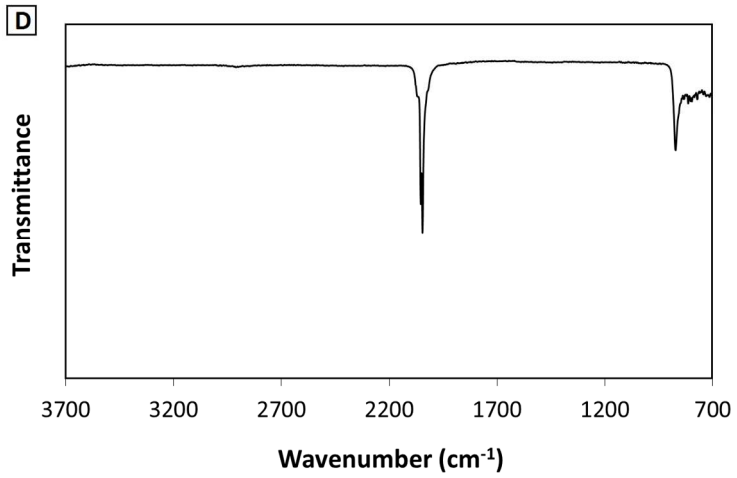

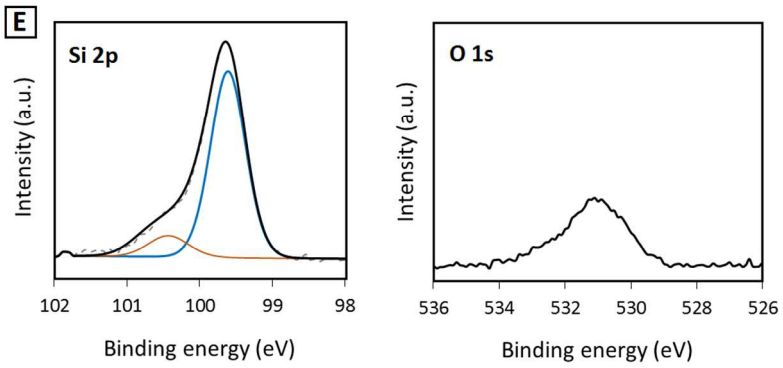

Figure S3. FT-IR spectra of 3 nm, 5 nm, and 8 nm Si-NCs after the (A) acetylferrocenium- and (B) 1,1'-diacetylferrocenium-activated methoxylation reaction.

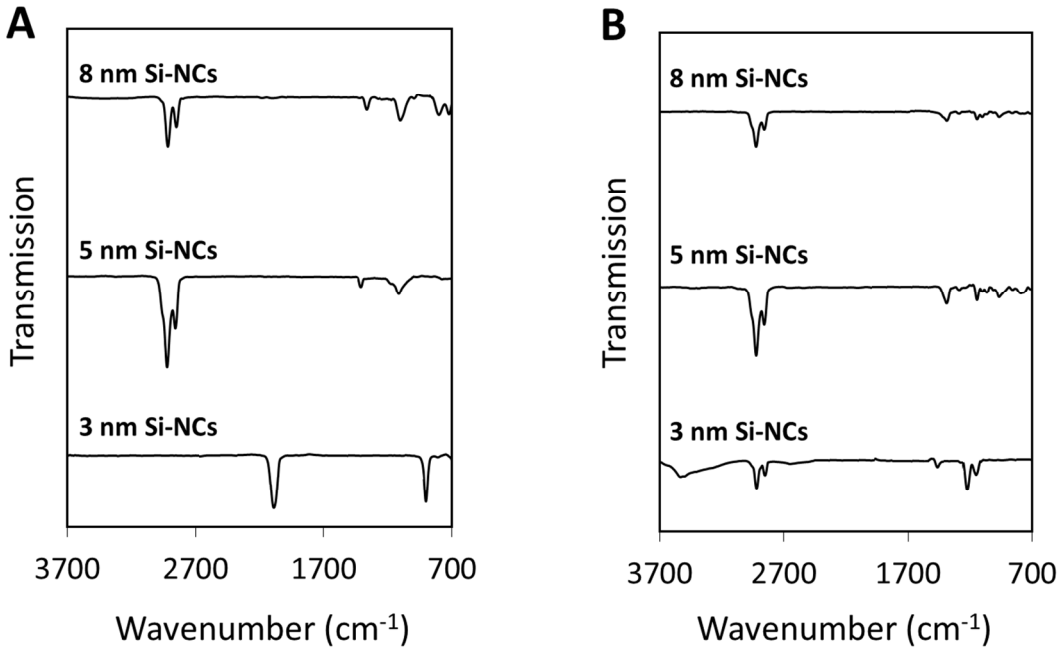

Figure S4. PL spectra 3 nm (blue line), 5 nm (green line), and 8 nm (red line) of methoxylated Si-NCs with λ_{ex} = 325 nm.

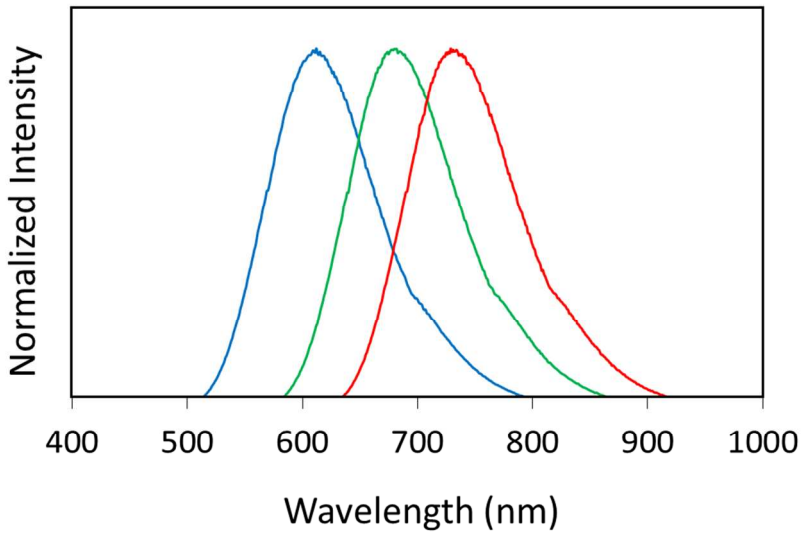

Figure S5. FT-IR spectrum of butoxy-functionalized Si-NCs.

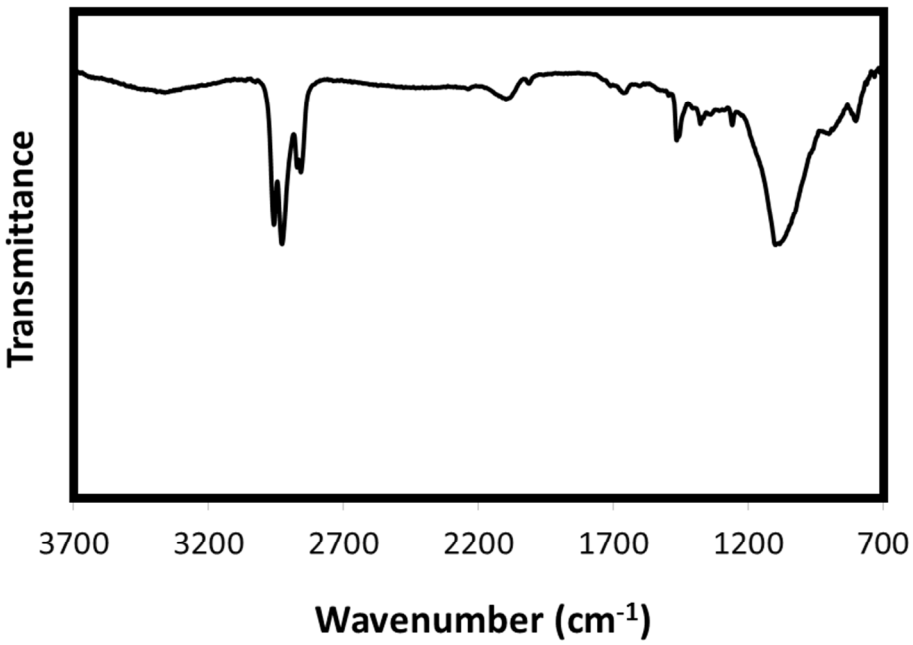

Figure S6. FT-IR spectrum of hydrogen-terminated Si-NCs reacted with butanol in the absence of ferrocenium.

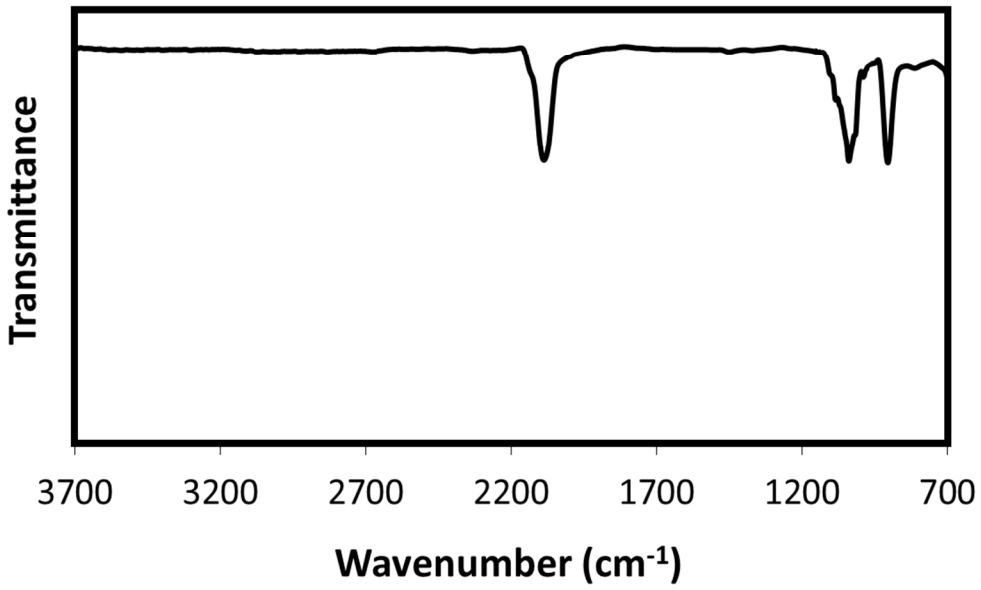

Figure S7. FT-IR spectrum of butylamine-functionalized Si-NCs.

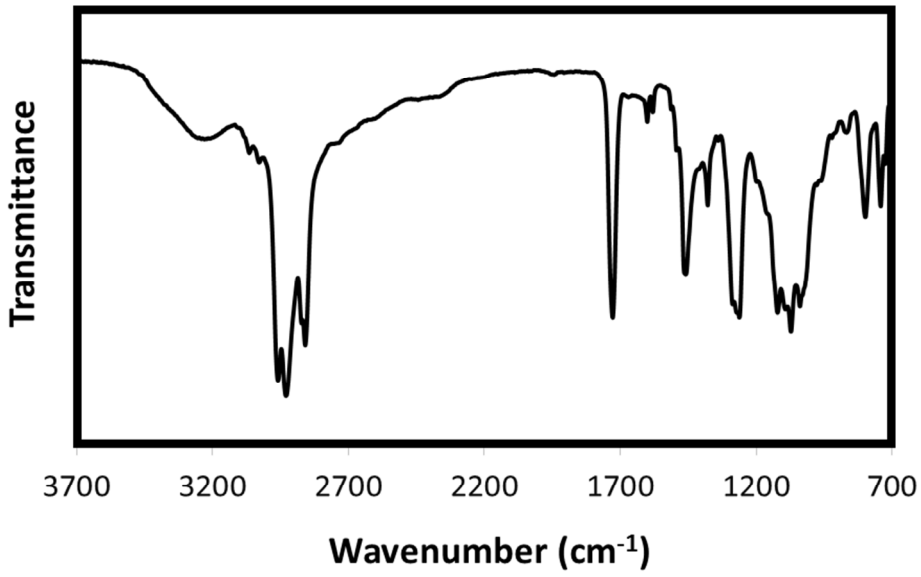

Figure S8. FT-IR spectrum of hydrogen-terminated Si-NCs reacted with butylamine in the absence of ferrocenium.

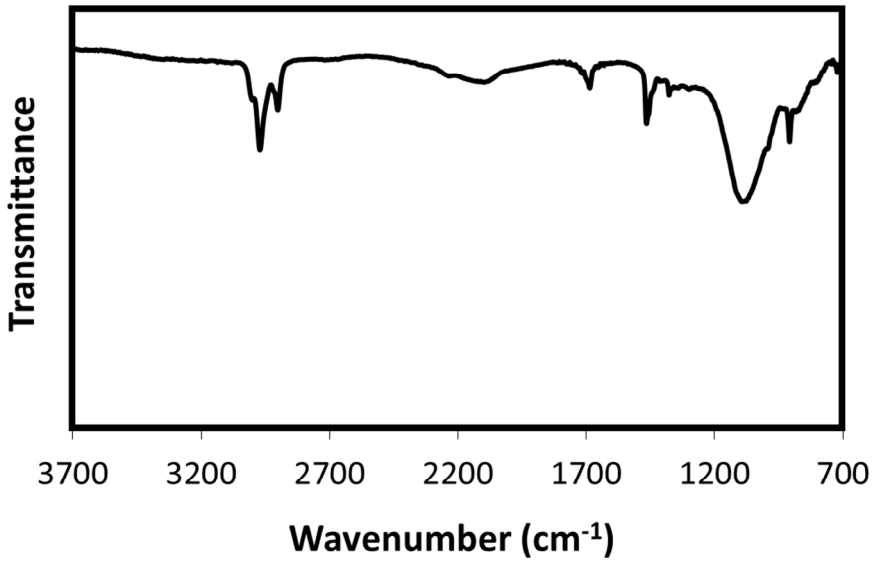

Figure S9. FT-IR spectrum of butanoic acid-functionalized Si-NCs.

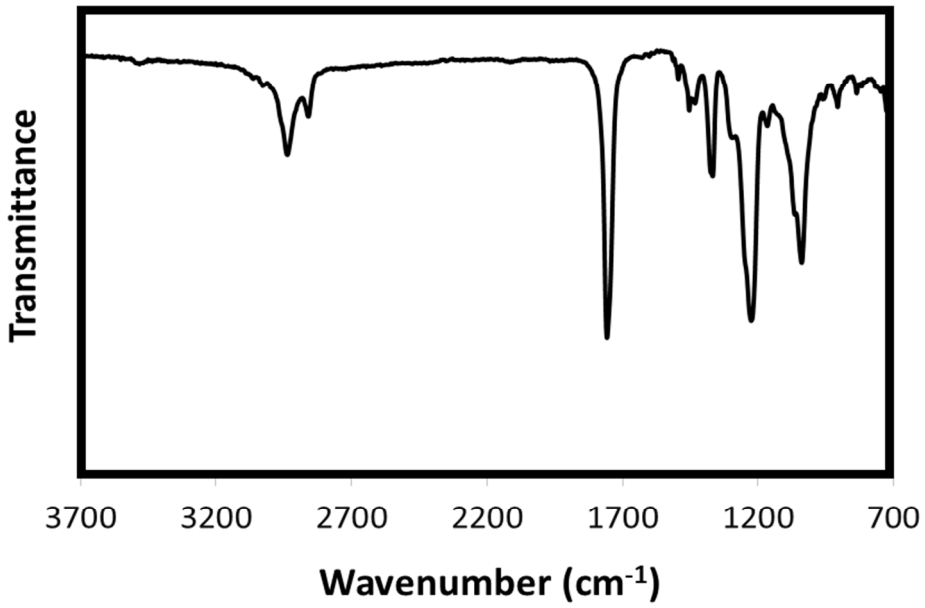

Figure S10. FT-IR spectrum of hydrogen-terminated Si-NCs reacted with butanoic acid in the absence of ferrocenium.

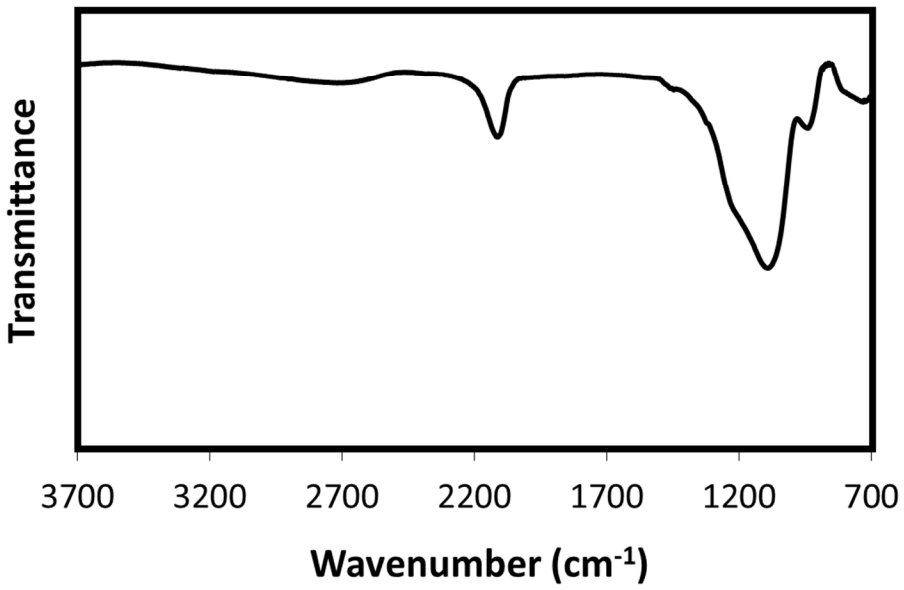

Figure S11. FT-IR spectrum of butylthiol-functionalized Si-NCs.

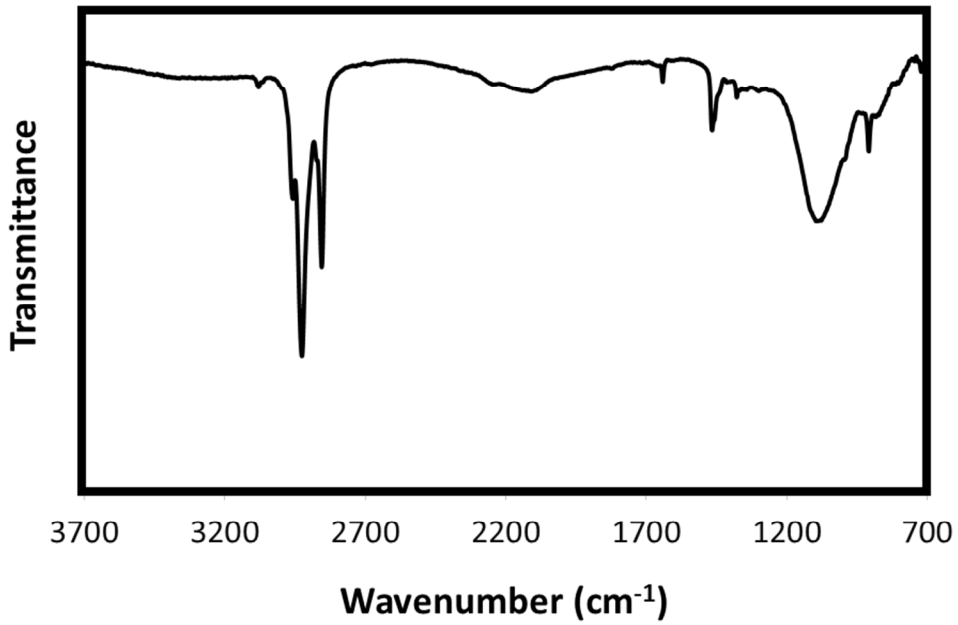

Figure S12. FT-IR spectrum of hydrogen-terminated Si-NCs reacted with dibutyl disulfide in the absence of ferrocenium.

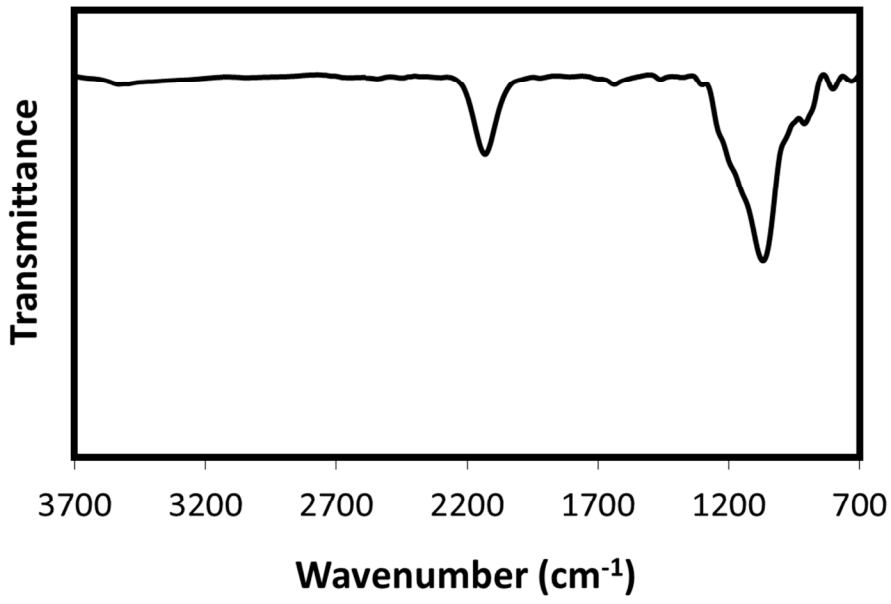

Figure S13. FT-IR spectrum of diethyl phosphine-functionalized Si-NCs.

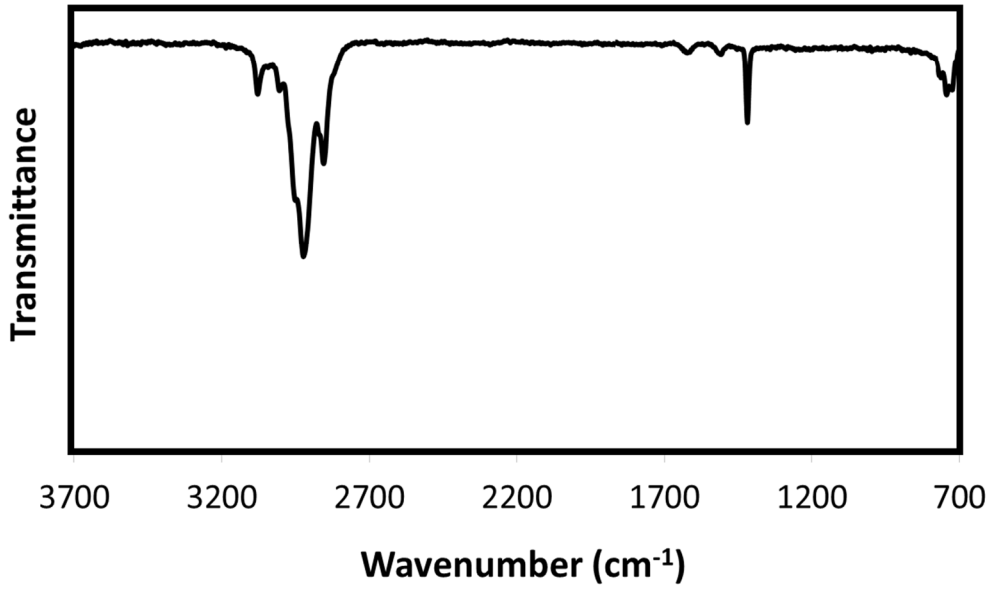

Figure S14. Photographs of phosphine-stabilized Si-NCs in hexanes, before (left) and after (right) exposure to air.

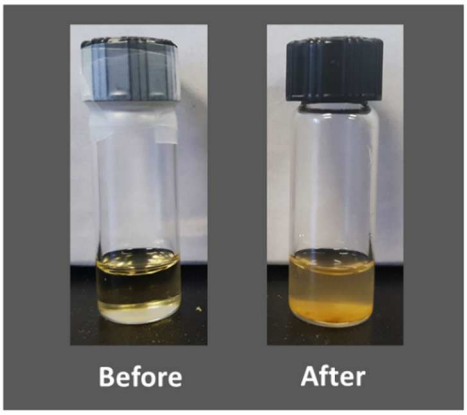

Figure S15. FT-IR spectrum of hydrogen-terminated Si-NCs reacted with diethyl phosphine in the absence of ferrocenium.

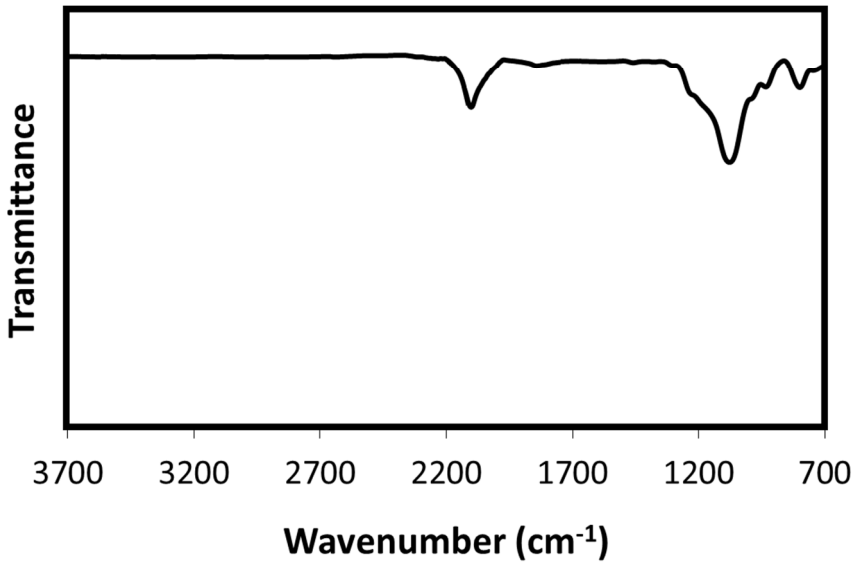

Figure S16. PL spectra of hydrogen-terminated 3.1 nm (blue line), 5.2 nm (green line), and 8.0 nm (red line) Si-NCs with λ_{ex} = 325 nm.

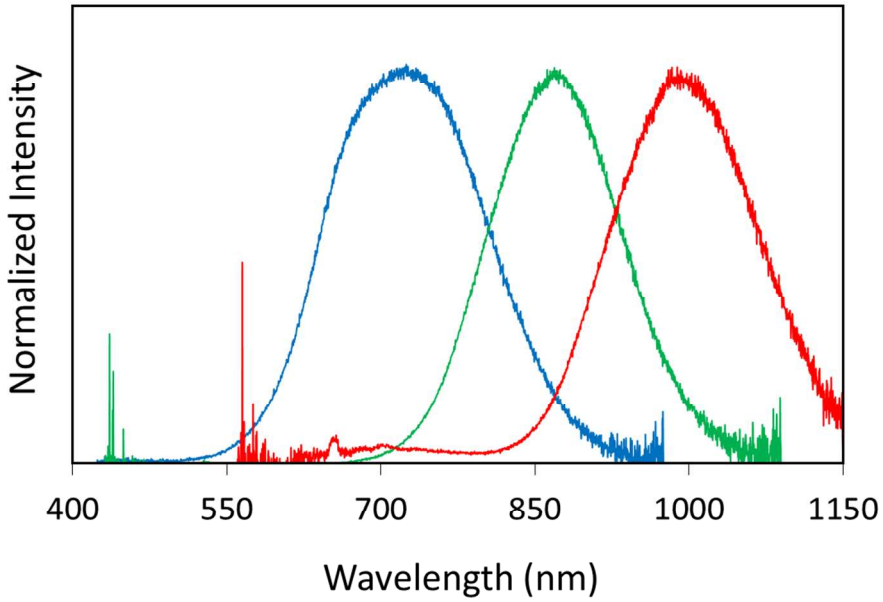

Figure S17. Photographs of butylamine-stabilized Si-NCs in THF, two weeks after functionalization. The NCs on the left were functionalized in the presence of ferrocenium whereas the NC's in the photo on the right were reacted in absence of ferrocenium.

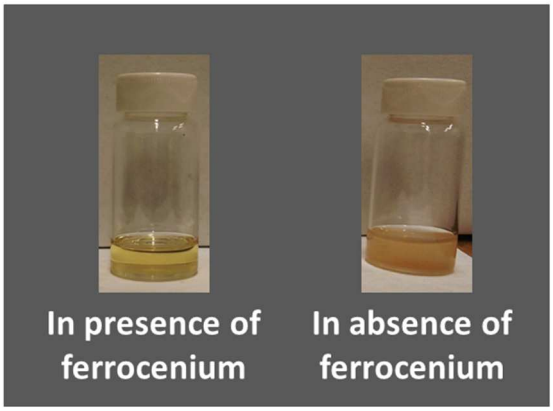

Figure S18. HR XP spectra of O 1s region of (A) butylthiol, (B) butylamine, and (C) diethylphosphine functionalized Si-NCs. The peaks are normalized for same counts.